

Protandrous Hermaphroditic Reproductive System in the Adult Phases of *Mothocya renardi* (Bleeker, 1857) (Cymothoidae: Isopoda: Crustacea) – Light and Electron Microscopy Study

Panakkool Thamban Aneesh¹ and Sudha Kappalli^{1,2,*}

¹Post Graduate Department of Zoology and Research Centre, Sree Narayana College, Kannur- 670 007, India.
E-mail: anee3716@gmail.com (Aneesh)

²Department of Zoology, School of Biological Sciences, Central University of Kerala, Kasaragod- 671320, Kerala, India.
*Correspondence: E-mail: sudhakappalli@cukerala.ac.in (Kappalli)

Received 5 May 2020 / Accepted 23 September 2020 / Published 23 November 2020
Communicated by Benny K.K. Chan

The reproductive system of *Mothocya renardi* (Bleeker, 1857), a protandrous hermaphroditic cymothoid that infects the belonid fish *Strongylura leiura* Bleeker, 1850, is characterized using light and electron microscopy. Three protandrous hermaphroditic adult phases are identified: male, transitional and female. Each phase includes a paired reproductive system, one on either side of the gut. Each consists of three lobed testes, followed by an ovary, then a vas deferens that opens into a penis on the same side. During the male phase, all testis lobes are filled with germ cells at various stages of spermatogenesis and spermeogenesis. Primary and secondary spermatogonial cells are confined to the peripheral side of the testis lobe. The ovary shows peripheral germarium and a large number of yolkless oocytes encircled by follicle cells. The oviduct emerged from the ovary mid laterally and its distal end was found to be sealed. The exceptionally elongated spermatozoon consists of a head and a long filamentous tail. The spermatozoa are found organized into characteristic bundles to form spermatophores, and these are also packed in the vas deferens during the male phase. During the transitional phase, on the other hand, testes appear to be withered, but the vas deferens contains spermatophores. The ovary shows yolky oocytes encircled by follicle cells. During the female phase, the testis lobes appear as thin, empty, and sac like, and the extremity of the vas deferens is closed. Ovaries contain yolky oocytes and more prominent oviducts than male and transitional phases. The present paper also discusses the pattern of correlation between 1) the ovarian and brood cycles and 2) the ovarian and molt cycles.

Key words: Protandrous hermaphroditism, Spermatophores, Oocytes, Follicle cells, Ovary cycle.

BACKGROUND

Isopoda, a crustacean order, comprises over 10,000 species living in diverse habitats, 45% of which are marine organisms that are free living or parasitic. While the majority of the crustacean parasites

are dioecious (*i.e.*, have separate male and female sexes), parasitic isopods display both protandrous and protogynous hermaphroditism. Protandrous sex changes have primarily been reported in parasitic isopods like epicarids and cymothoids (Cressey 1983; Brook et al. 1994; Cook and Munguia 2015; Smit et al. 2019;

Aneesh et al. 2018). If males of the cymothoid *Anilocra frontalis* H. Milne Edwards, 1840 happen to infest the host fishes *Labrus bergylta* Ascanius, 1767 and *L. maculatus* Bloch, 1792 solitarily, it may transition or develop into a functional female. On other hand, if another male settles into the same host as this female, the new male remains the same gender until the female dies or is removed (Legrand 1952).

Most studies on the structure of isopod reproductive systems are focused on free living and non-hermaphroditic forms. In *Saduria entomon* (L.), a marine and free-living isopod, for instance, spermatogenesis does not appear in a synchronized pattern in their testis tubules because the germ cells display different levels of maturation and stay associated with the somatic cells (Hryniewiecka-Szyfter and Tyczewska 1991). In *Oniscus asellus* (L.) and *Armadillidium vulgare* (Latreille 1804), accessory cells produce extracellular tubules surrounding the spermatozoa in spermatophores (Reger and Fain-Maurel 1973; Itaya 1979). Free-living isopods have also been shown to have a unique type of spermatozoon, consisting of a cell body enclosing a long ribbon-like nucleus, above which an acrosomal complex and a long flexible tail are found (Cotelli et al. 1976; Reger et al. 1979). In the females of *Saduria entomon* (L.) and *Asellus aquaticus* (L.), the oviduct is modified into a sperm reservoir (Hryniewiecka-Szyfter and Babula 1995; Erkan 1998).

Though protandrous hermaphroditism has been reported in epicarids and cymothoids (Brusca 1981; Brook et al. 1994), these studies are based on morphological evidence and little is known about the histological and physiological characteristics associated with hermaphroditism in this group (Brook et al. 1994; Poulin 1995; Kottarathil and Kappalli 2019a b). In the cymothoid *Ichthyoxenus fushanensis* Tsai and Dai 1999, protandrous hermaphroditism is reportedly associated with a sexual size dimorphism, with females being much larger than males, and the presence of vestigial penes (Tsai and Dai 1999; Tsai et al. 1999). In *Ceratothoa oestroides* Risso, 1816, *Nerocila orbigny* (Guerin-Meneville, 1832), *N. bivittata* Risso, 1816, *Anilocra physodes* (L.), *A. mediterranea* Leach, 1818, and *Norileca indica* H. Milne Edwards, 1840, the gonad appears with the ovary and testis, along with their ducts (Kottarathil and Kappalli 2019a b). The general anatomy of the protandrous hermaphroditic gonad of *N. indica*, a host-specific cymothoid that infects the scombrid fish *Rastrelliger kanagurta* (Cuvier, 1816), has been characterized (Kottarathil and Kappalli 2019a b). Despite these few reports, information on the hermaphroditic reproductive system and its pattern of functioning in parasitic isopods is still incomplete.

Cymothoids exhibit both obligatory parasitism and protandrous hermaphroditism, so their reproductive system needs to be structurally characterized based on different hermaphroditic life cycle stages by considering more cymothoid genera and species. At this juncture, this study is relevant because it reports the organization of the hermaphroditic reproductive system in male, transitional, and female phases of a cymothoid, *Mothocya renardi* (Bleeker, 1857), using light and electron microscopy. *Mothocya renardi* infects the belonid fish species *Strongylura leiura* Bleeker, 1850 along the Malabar coast (Kerala, India) in a single-host-specific manner with high prevalence (92%) (Aneesh et al. 2016). The present paper also demonstrates correlations between the 1) ovarian cycle and brood cycle and 2) ovarian cycle and molt cycle. This basic information will be helpful for understanding the importance of protandric hermaphroditism, if any, to the obligatory parasitic life of cymothoids.

MATERIALS AND METHODS

Sample Collection

Live samples of adult life cycle phases of *Mothocya renardi* (Bleeker, 1857) parasitizing the fish *Strongylura leiura* Bleeker, 1850 were collected from the Ayyikkara fish landing center (Lat. 11°51'N, Long. 75°22'E; Malabar Coast, India). Sampling was performed weekly, and soon after collection, the live parasites were brought to the laboratory and maintained in a plastic cistern containing sea or estuarine water. Parasites without a host were found to live for a maximum of six hours. The live samples were observed and processed for further study. The adult male ($n = 301$; 10.0–19.0 mm), ovigerous female ($n = 335$; 16.0–34.0 mm), and transitional phases ($n = 39$; 10.5–23.0 mm) were identified according to Aneesh et al. (2016).

Dissection and photomicrography

Mothocya renardi hermaphroditic reproductive system from each adult life cycle phase (male, transitional, and female) was dissected by cutting open the thoracic sternites under a stereomicroscope (Leica-S6D), then quickly rinsing it in sea or estuarine water and placing it on a clean glass slide. Photomicrography was performed using a Leica Stereo Zoom -S6 D with a Canon Power Shot S 50 camera attached and processed with the software LAS EZ (Leica Application Suit-Version 1.7.0). The tissue was then closely observed for morphological characterization under a

stereomicroscope (Leica S6) and processed for further histological and ultrastructural studies following Kottarathil and Kappalli (2019a b)

Identification of ovarian stages

The ovary of female-phase *M. renardi* was classified into seven stages based on the oocyte size: a Pre-vitellogenic stage (Pvs), five Vitellogenic stages (Vg1–Vg5), and a Spent stage (Ss).

Identification of molt and brood stages

The maxillule was used to identify the molt stages following the procedure described by Aneesh and Kappalli (2020). Brood stages such as Zygotic stage, Embryonic stages (ES I/ES II/ES III), and larval stages (Manca-1 and Manca-11) were classified according to Aneesh et al. (2016).

Histology

The dissected reproductive systems (consisting of testis, ovary, and vas deferens, along with their respective ducts) from male, transitional, and female phases of *M. renardi* were immediately fixed in Carnoy fixative (mixture of ethanol and acetic acid in the ratio of 3:1); microtome (paraffin) sections 3–5 μm thick were stained in Harris haematoxylin-eosin (after Pearse 1968). DPX (Merck) mounted slides were observed under the Leica Research Microscope (DM 750), and photomicrography was performed using a Leica ICC50 camera attached; the microscopic images were processed with the software LAS EZ (Leica Application Suit-Version 1.7.0).

Electron microscopy

The dissected tissues (ovary, testes, and vas deferens of the male phase and ovary of the female phase of *M. renardi*) were fixed in Karnovsky's fixative (4% paraformaldehyde and 3% glutaraldehyde at pH 7.2) for 24 h, then processed following the procedure described by Williams and Carter (1997). The tissue was washed twice in phosphate buffer (pH 7.4) for 15 minutes and subsequently post-fixed in 1% osmium tetroxide. After washing (with phosphate buffer, pH 7.4) and dehydrating, the tissue was transferred to an enblock stain (2% uranyl acetate in 95% ethyl alcohol), followed by dehydration and clearing. Then the tissue was embedded in araldite. Semithin (1.0 μm) and ultrathin (0.5 μm) sections were cut using a Leica Em Uc6 ultra microtome fixed with a glass knife and placed in glass slides and copper grids, respectively.

The semithin sections stained with methylene blue were used for the light microscopic observation. The ultrathin sections mounted in the copper grid were stained with Uranyl acetate followed by lead citrate. The stained specimens were subjected to observation under a Transmission Electron Microscope (Tecnai G2) in the NIMHANS facility (Bangalore).

Correlation between stages of ovary cycle and brood cycle

The stages of the ovary cycle and stages of the brood cycle of female-phase *M. renardi* were closely observed individually ($n = 34$) to assess the correlation, if any, between these cycles.

Correlation between ovary cycle and biphasic molt cycle

The ovary and molt cycle stages of female-phase *M. renardi* were closely observed individually ($n = 42$) to assess correlation, if any, between these cycles.

Statistical analysis

The mean value was calculated using the standard statistical software InStat (Graphpad InStat, Version 2.00, 2007).

RESULTS

Reproductive system of the male-phase *M. renardi*

Gonads and gametes: light microscopic observations

The paired and symmetrical reproductive system of *M. renardi* is located dorsally on either side of the gut, and each consisted of three testis lobes, one ovary, and their respective ducts (vas deferens and oviduct) (Fig. 1A). The testis lobes and ovary appeared to be closely associated structures, and the ovary formed a simple tubule 1850–2300 μm long and 350–500 μm wide. Three testis lobes were positioned at the antero-lateral border of the ovary (Fig. 1A). The spermatozoa were organized in bundles to form spermatophores (Fig. 1B–D), each of which contained 84.57 ± 14.99 ($n = 6$) spermatozoa organized in such a way that spermatozoan tails aligned parallel to the long axis of the bundle (Fig. 1D). Mature spermatozoon appeared as an elongated structure consisting of a head containing a ribbon shaped nucleus and a long filamentous non-

motile tail 0.06 ± 0.001 mm and 1.35 ± 0.25 mm long, respectively. The sperm head contained the nucleus; the bulb-like acrosome connected the head and tail (Fig. 1F).

Gonads and gametes - Histology and ultrastructure

Testis and germ cells

Each testis lobe of *M. renardi* was composed of germ cells undergoing spermatogenesis and somatic accessory cells (Figs. 2, 3). The testis wall was composed of a basal lamina supported by connective tissue and a muscle layer (Fig. 2A–C). All germ cells occupying a particular region of the testis lobe were at the same stage of development (Fig. 2A). The differentiated primary and secondary spermatogonia cells were found confined to the periphery of the testis. Relatively large primary spermatogonia were 12.02 ± 0.08 μm in width and their spherical large nuclei were characterized by peripherally distributed condensed chromatin and one or two centrally located nucleoli (Fig. 2F). Secondary spermatogonia measured 9.05 ± 0.04 μm in width, had less cytoplasm than the primary

one, and had a nucleus with scattered chromatin and a prominent nucleolus (Fig. 2B, F). Spermatocytes (Figs. 2A–D, 3A, 4A1) measured 7.95 ± 0.08 μm in width and appeared under different divisional stages, mostly meiotic prophase and metaphase (Figs. 2B, 3A).

The spermatids (Fig. 3B–D) were relatively small (4.92 ± 0.1 μm in width) and highly distinct from other developing germ cells. Those under more advanced stages of spermiogenesis lay close to the somatic accessory cells lying marginal to the testis wall (Fig. 3B–E). Under the electron microscope, the chromatin-rich nucleus of the spermatids appeared to be highly electron-dense (Fig. 4A2). In the longitudinal section, the sperm tail appeared as an elongated structure showing transverse striations and a central lumen filled with electron-dense material (Fig. 4D1–3). The outer margin of the tail was covered with a double-layered membrane (Fig. 4D3). The ultrastructural view showed that the spermatophore also contained an abundance of massive extracellular tubules (Figs. 4B3, 4C3, 4D1). The wedge-shaped acrosome appeared to be highly electron-dense (Figs. 4B1–2, 4C1–3). The cytoplasmic area between the acrosome and nucleus contained mitochondria (Fig. 4B2).

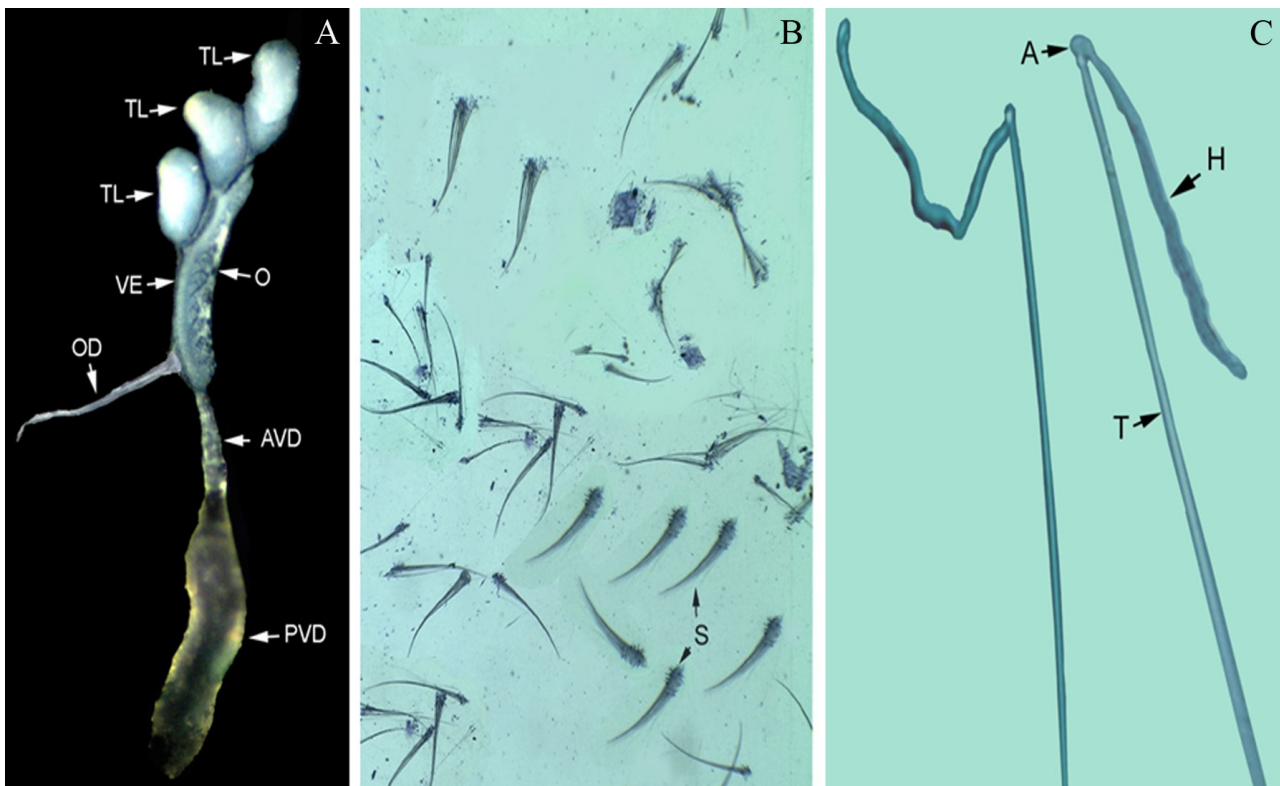


Fig. 1. *Mothocya renardi* (Bleeker, 1857): Reproductive system during the male phase. A, Hermaphroditic reproductive system showing testis lobes, ovary, vas deferens, and oviduct (4X); B, spermatozoa: unstained (10X); C, spermatozoa: unstained (100X). O: ovary, TL: testis lobe, VE: vas deferens, OD: oviduct, AVD: anterior vas deferens, PVD: posterior vas deferens, S: spermatophore, T: tail, A: acrosome, H: head.

Ovary and germ cells

The histological sections of the ovary of male-phase *M. renardi* showed a narrow channel running along its lateral margin and lumen with an abundance of small oocytes with a prominent nucleus and one or two nucleoli (Fig. 5A–B). Each oocyte was encircled by a layer of follicle cells (Fig. 5A–B).

Vas deferens

Both anterior and posterior vas deferens of male-phase *M. renardi* had many spermatophores resembling those found in the testis lobe. In the electron microscopic view, the lumen of the vas deferens had an abundance of extracellular tubules, and their density was higher in the vas deferens than the testis lobe (Fig. 6A–C).

Reproductive system in the transitional-phase *M. renardi*

During the transitional phase, the sac like testis lobes appeared withered and occasionally contained

several spermatophores (Fig. 7A). Histologically, the posterior part of the vas deferens was filled with spermatophores (Fig. 7B), but its posterior extremity was sealed throughout this phase. Histologically, the ovary showed the presence of relatively large oocytes with a nucleus and one or two nucleoli; each oocyte was encircled by a follicular layer (Fig. 7C). Though the oviduct was relatively wider than that found during the male stage, its extremity remained sealed throughout the transitional phase.

Ovary in the female-phase *M. renardi*

The kidney-shaped ovary consisted of 8–10 cone-shaped pouches, each containing 42–62 oocytes (Fig. 8C). During the Pvs (previtellogenic stage), the relatively small ovary contained a large number of proliferating oocytes ranging from 1–150 μm long (Fig. 9A), each with a large nucleus and nucleolus. The wall of the previtellogenic ovary contained highly branched foldings throughout its length (Fig. 10A and B). During the vitellogenic stages (Vg1–Vg5), the ovary contained yolky oocytes—as was evident by the presence of highly basophilic yolk globules—which showed a

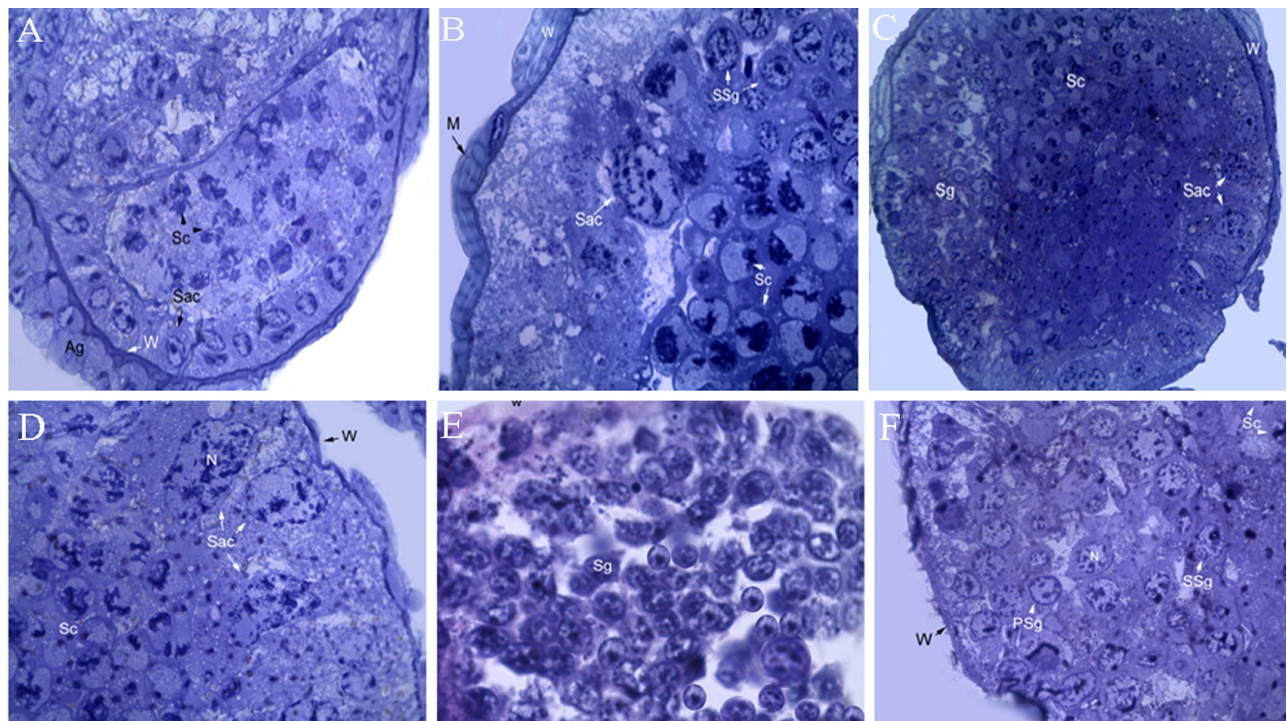


Fig. 2. *Mothocya renardi* (Bleeker, 1857): Testis lobe during the male phase. A–D, Semithin sections (CS; 1 μm : toluidine blue stained). A, Acini and androgenic gland (100X); B, wall showing muscle band (100X); C, somatic accessory cells and germ cells during different stages of maturation (40X); D, enlarged view showing somatic accessory cells (100X). E, Histological section (CS; 4 μm : haematoxylin-eosin) showing spermatogonial cells (100X). F, Primary and secondary spermatogonia (100X). Sc: spermatocytes, Sac: somatic accessory cell, W: wall, Ag: androgenic gland, M: muscle layer, SSg: secondary spermatogonia, Sg: spermatogonia, N: nucleus, Psg: primary spermatogonia.

concomitant increase in number from Vg1 through Vg5; the oocytes contained a visible nucleus and nucleolus, and each oocyte was encircled by a layer of follicle cells throughout all the stages (Fig. 9B–E). The oviduct (Fig. 8A and C) arising from the posterolateral margin of each

ovary was opened at the 6th thoracic segment. After oviposition, the spent staged (Ss) ovary appeared as an opaque and flaccid structure containing few residual eggs (Fig. 8F). Histologically, the Ss ovary contained residual follicle cells of the preceding clutch of oocytes

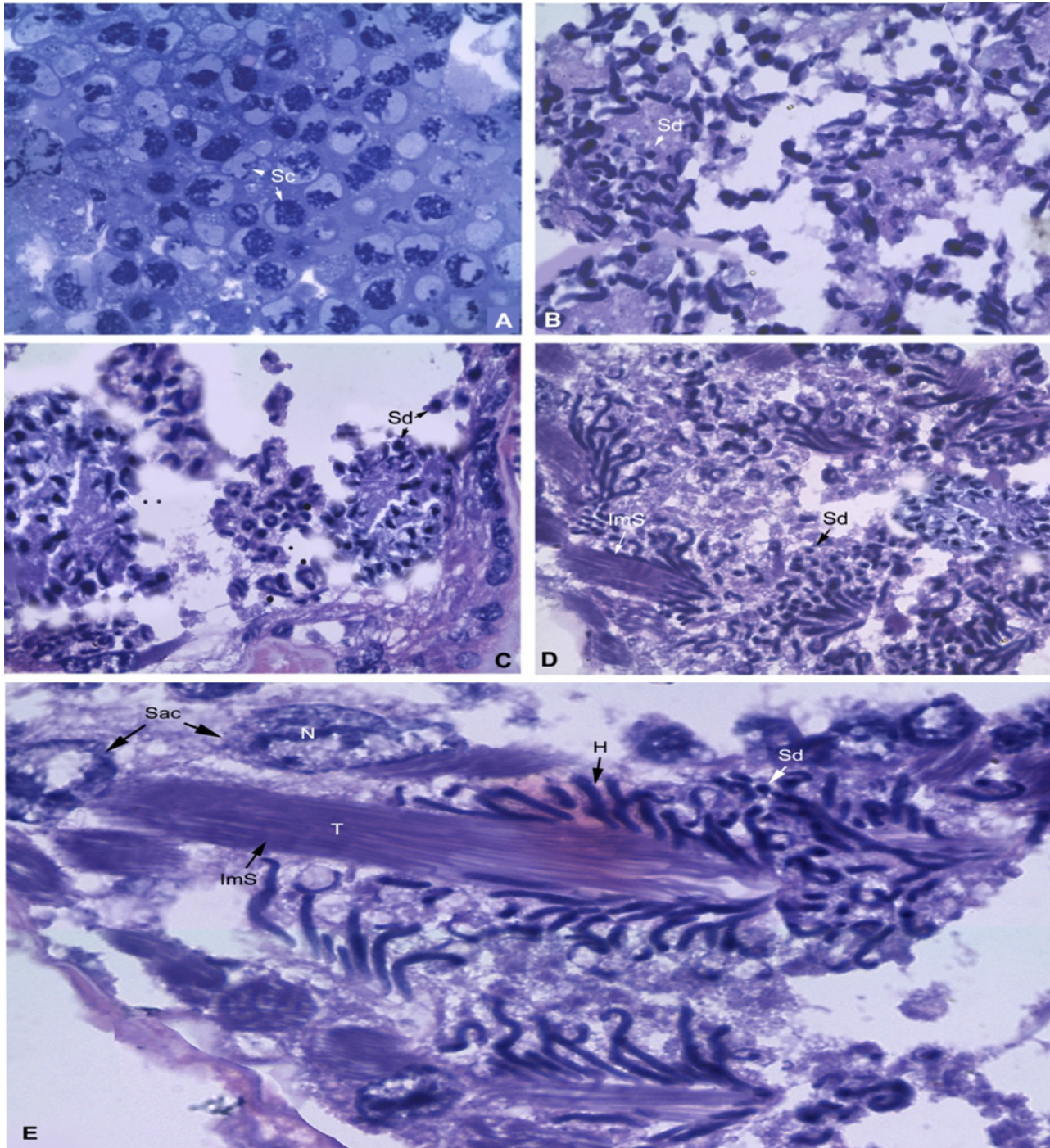


Fig. 3. *Mothocya renardi* (Bleeker, 1857): Histology of testis lobes during the male phase. A, Semithin section (LS; 1 μ m: toluidine blue) showing spermatocytes during meiotic division. B–E, Cross sections (4 μ m: haematoxylin-eosin) showing the spermatids during different maturation stages. Sc: spermatocytes, Sd: spermatid, ImS: immature spermatozoa, T: tail, N: nucleus, H: head, Sac: somatic accessory cell.

(Fig. 9F).

Correlation between ovarian cycle and brood development in *M. renardi* during the female phase

While the female *M. renardi* was brood carrying, a second clutch of oocytes started developing in the ovary. Interestingly, the stages in the succeeding ovarian cycle showed a perfect synchrony with the brood development (Fig. 11A). Immediately after oviposition, the spent stage ovary appeared as an opaque, thin, and flaccid structure; the eggs remained in the brood pouch during the zygotic stage (uncleaved stage). While the

ovary was in the Pvs, eggs in the marsupium completed cleavage and reached any of the three embryonic stages (ES I/ES II/ES III). When the ovary entered the Vg1, the ES III-stage eggs in the marsupium hatched into the first larvae, Manca-1. When the ovary reached Vg2, the brood pouch of the mother animal contained the next stage of larvae, Manca-II, or was empty (after releasing the Manca-II). When the female molted to remove the old brood pouch, oocytes were at Vg3. No brood pouch was found in females, while their ovary was at stage Vg5. When the ovary reached late Vg5 (oocytes 1230 μm in width), the female possessed a partially or completely formed brood pouch to receive the next clutch of eggs.

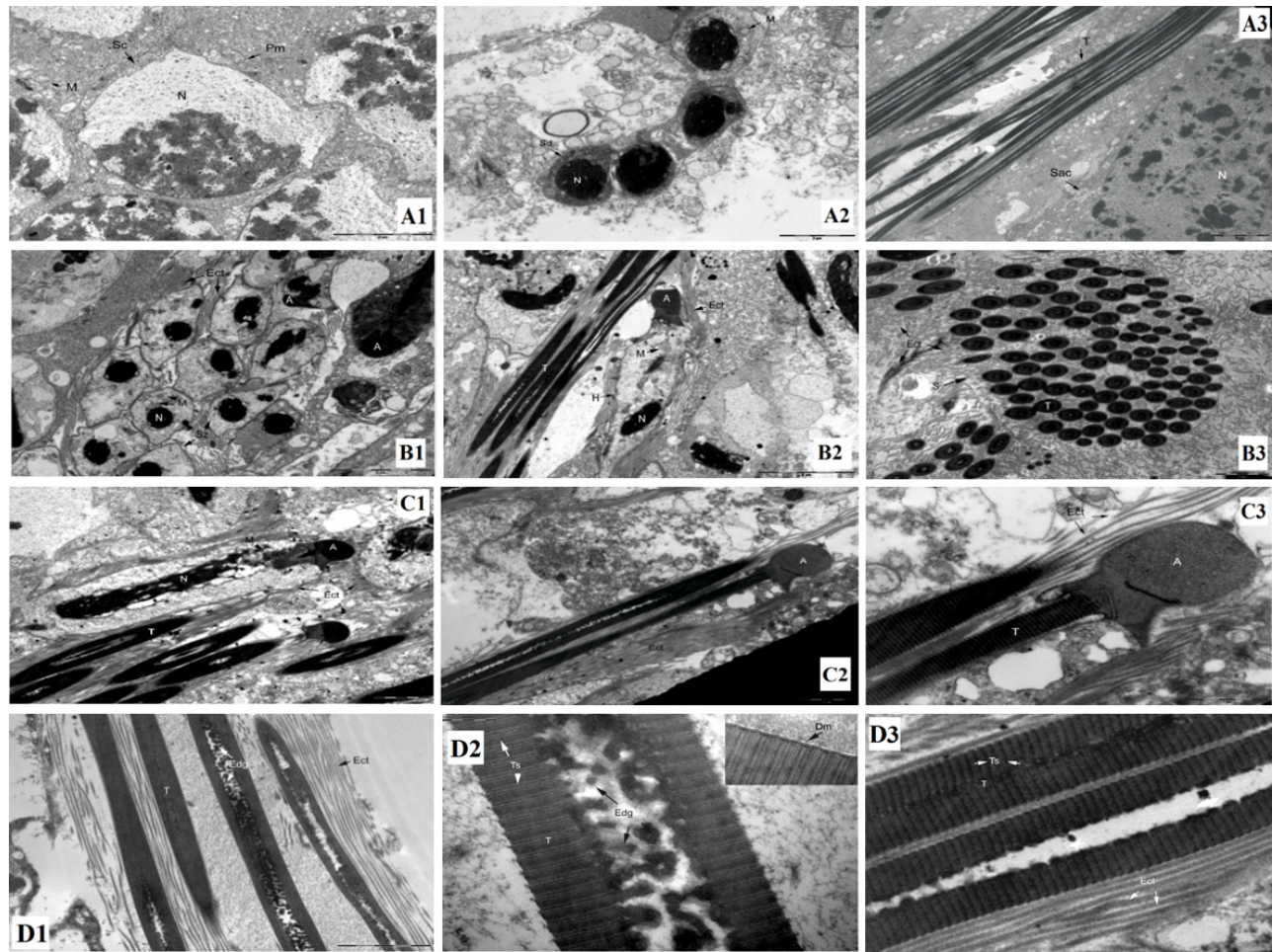


Fig. 4. *Mothocya renardi* (Bleeker, 1857): Electron micrograph of the testis lobes during the male phase: A1, Spermatocyte (4800X); A2, spermatids (9300X); A3, somatic accessory cells and portion of spermatophore (2900X); B1, cross section through spermatozoan head (4800X); B2, longitudinal section through spermatophore (4800X); B3, cross section through spermatozoan tail (6800X); C1, spermatozoan head region (6800X); C2, spermatozoan tail, acrosome and extracellular tubules (6800X); C3, spermatozoan acrosome and tail (18500X); D1, spermatozoan tail surrounded by extracellular tubules (11000X); D2, spermatozoan tail (30000X) showing transverse striations and central lumen (insight: wall of spermatozoan tail with double membrane); D3, a portion of spermatozoan tail showing central lumen filled with electron-dense granules (68000X). Sc: spermatocyte, N: nucleus, M: mitochondria, Pm: plasma membrane, Sd: spermatid, T: tail, H: head, Sac: somatic accessory cell, A: acrosome, Ect: extracellular tubule, Sz: spermatozoa, S: spermatophore, Edg: electron-dense granules, Ts: transverse striations, Dm: double membrane.

Correlation between ovary cycle and biphasic molt cycle in *M. renardi* during the female stage

In *M. renardi* each ovary cycle was accompanied by two molt cycles (one to remove the old brood pouch and the other to form the new brood pouch) (Fig. 11B). Furthermore, we found a correlation between the molt stages and ovary stages of *M. renardi*. When the ovary was at the Ss/Pvs/Vg1 stages, the female remained in the intermolt stage. As the ovary stage advanced to Vg2, the female reached the early premolt stages (D₀–D₂) at its posterior part. When the ovary stage reached Vg3, the parasite entered late premolt stages (D₃/D₄) at its posterior part or completed the ecdysis (of posterior body part). During the period between Vg4 and Vg5, the parasite completed the ecdysis of the anterior body part. By the end of this biphasic molt cycle, the old brood pouch had disappeared and the individual entered into the second molt cycle (to form the new brood pouch). When this molting process was over, the females were

found to have an ovary at Vg5. Oviposition ensued when the females reached the intermolt stage.

DISCUSSION

Isopods use different modes of reproduction and mating strategies, and these have been explored widely in free living forms (Shuster and Wade 1991 2003). Parasitic isopods like epicarids and cymothoids display protandrous hermaphroditism, and the underlying transitions from male to female phases are critical for these parasites. In all three identified hermaphroditic sexual forms of *M. renardi* (male, transitional, and female), the paired and symmetrical gonad is intersexed and each consists of three testis lobes, an ovary, and ducts in the vas deferens and oviduct that lead to the respective gonopore. Throughout the male phase, the ovary contains yolkless oocytes with nuclei and more than one nucleolus, indicating that they are not in a

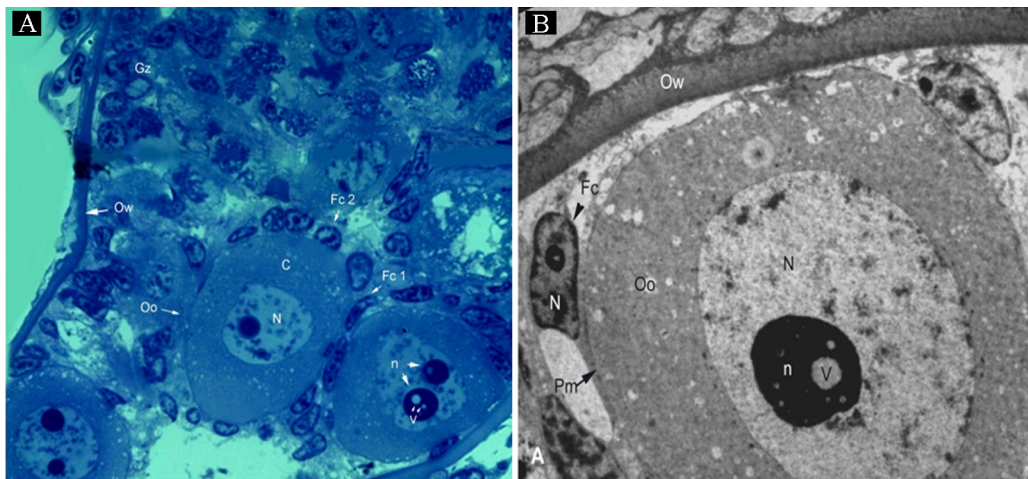


Fig. 5. *Mothocya renardi* (Bleeker, 1857): Ovary during the male phase. A, Semi thin section (LS; 1 μm; toluidine blue) showing germarium and previtellogenic oocytes encircled by follicle cells (100 X). B, Electron micrograph of ovary (LS; 0.5 μm) showing previtellogenic oocyte encircled by follicle cells (1400X). N: nucleus, n: nucleolus, Pm: plasma membrane, Oo: oocyte, Gz: germinal zone, Ow: ovarian wall, C: cytoplasm, Fc: Follicle cell, V: vacuole.

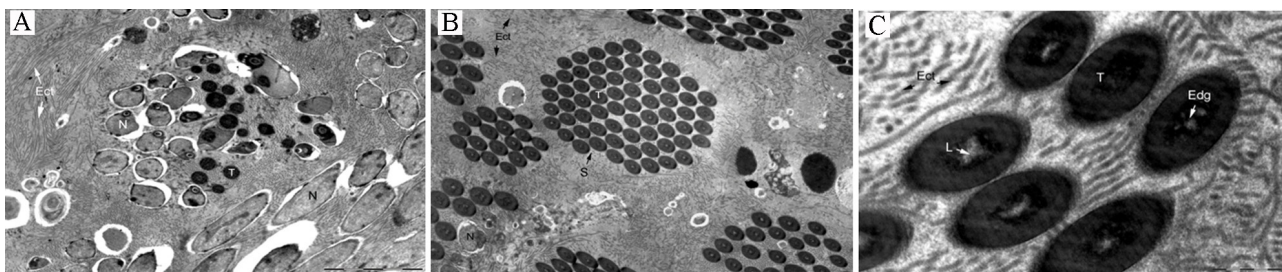


Fig. 6. *Mothocya renardi* (Bleeker, 1857): Electron micrographs of the cross sections of the vas deferens during the male phase showing spermatophore. A, Head regions (3200X); B, tail regions (6800X); C, tail regions showing central lumen with electron-dense granules (30000X). N: nucleus, T: tail, H: head, Ect: extracellular tubule, S: spermatophore, Edg: electron-dense granules, L: lumen.

dormant state (Fig. 11). When the male enters the transitional phase, oocytes increase in both number and size, and yolk deposition occurs. The transformation of the ovary from the previtellogenic stage into the vitellogenic stage through the transitional phase indicates that *M. renardi* undergoes a gradient of feminization, which agrees with the observations of the freshwater crayfish *Parastacus brasiliensis* von Martens 1869 (Almeida and Buckup 1997), the caridean shrimp *Samastacus spinifrons* Philippi, 1882 (Rudolph 1999), and the cymothoid *N. indica* (Kottarathil and Kappalli 2019a b). In *M. renardi*, when the members transform from the male to transitional phase through molting, gonopores (opening of oviduct and vas deferens) remain sealed and the penes become rudimentary, indicating

the termination of the male phase. The subsequent female phase contains the brood, and the ovary also contains yolky oocytes, while the testis lobe and vas deferens contain leftover spermatophores. The present morphological observation together with histological studies on the gonad of *M. renardi* confirm the existence of sequential protandrous hermaphroditism similar to that reported in *N. indica* (Kottarathil and Kappalli 2019a b) and *P. brasiliensis*, in which the protandrous hermaphroditic sexual stages are termed intersexed males, transitionals, and intersexed females. In another crayfish species, *Parastacus nicoleti* Philippi, 1882, the male gonad contains the previtellogenic ovary, but it is not distinct from the testis and appears as an ootestis (Rudolph 1999). Contrary to this pattern, in

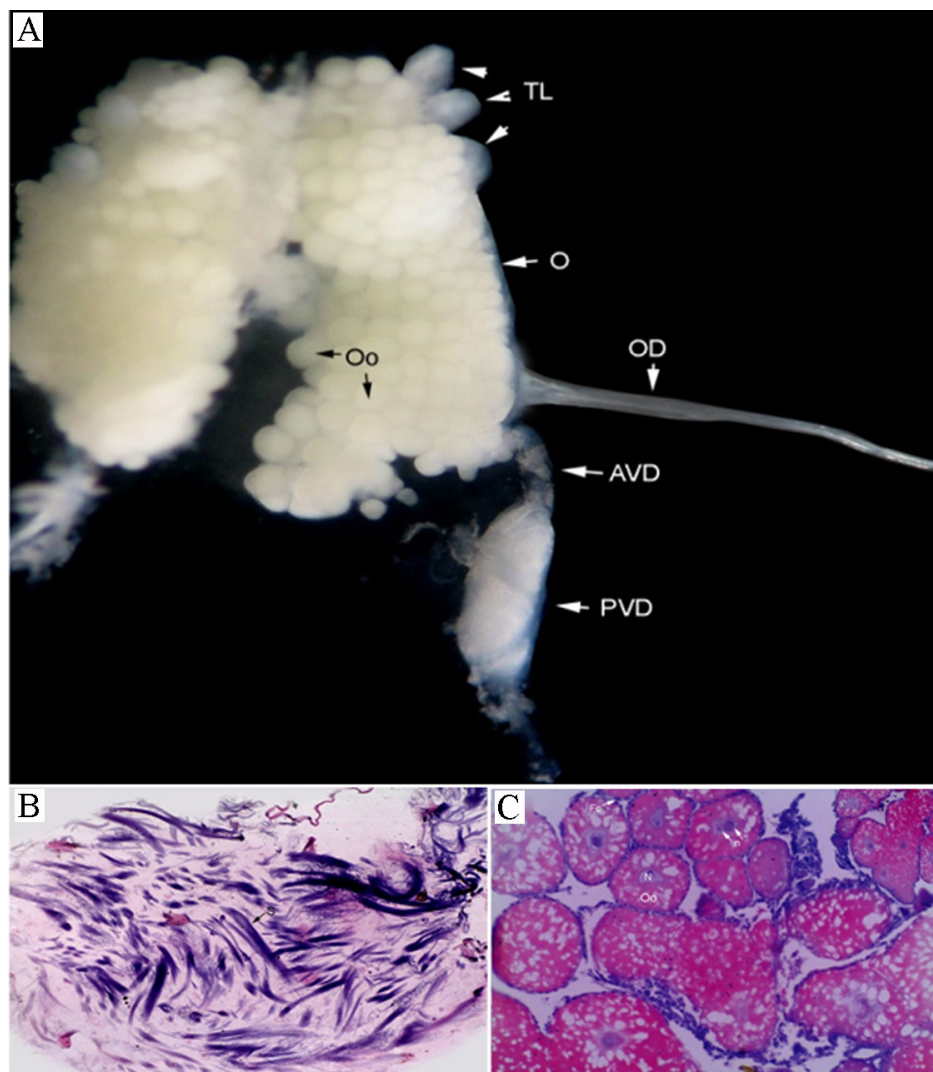


Fig. 7. *Mothocya renardi* (Bleeker, 1857): Reproductive system during the transitional phase. A, Reproductive system showing oocyte-filled ovary, spermatophore-filled vas deferens, and oviduct (4X); B, histological section (LS; 4 μ m; hematoxylin-eosin) through vas deferens showing spermatophores (20X); C, histological section (LS; 4 μ m; hematoxylin-eosin) through ovary showing yolky oocytes (20X). O: ovary, TL: testis lobe, OD: oviduct, AVD: anterior vas deferens, PVD: posterior vas deferens, Oo: oocyte, N: nucleus, n: nucleolus, Fc: follicle cell, S: spermatophore.

M. renardi (present study), the testis lobes appeared as the prominent ovarian diverticula, irrespective of the sexual stage, and it appeared more pronounced during the male stage, showing several acini, as is the case in *P. brasiliensis* (Almeida and Buckup 1997).

Histologically, each testis lobe of the male-stage *M. renardi* is composed of germinal cells at various stages of spermatogenesis and spermiogenesis, along with somatic accessory cells akin to those reported in *N. indica*. The wall of the testes is supported by connective tissue and a muscle layer forming the basal lamina, as found in the free-living isopod *Saduria entomon* (L.) and brachyuran crabs *Spiralothelphusa hydrodroma* (Herbst, 1794) and *Ranina ranina* (L.) (Minagawa et al. 1994). *Mothocya renardi* germ cells at the same stage of maturation form acini in a specific region of the testis. For instance, spermatogonia occupy the peripheral region of each testis lobe, and spermatocytes are found close to spermatogonia while the spermatids occupy more or less the center of the testis lumen. In *N. indica*, both primary and secondary spermatogonia usually occupy the periphery of the testis, irrespective of their lobes, and each lobe displays clusters of germ cells undergoing a specific stage of differentiation.

While one portion of the testis lobe has an abundance of spermatozoa/spermatophores, the remaining portion houses the germ cells undergoing spermatogenesis, of which meiotically dividing spermatocytes are dominant (Kottarathil and Kappalli 2019a). The present study also supports this observation. In the free-living isopod *S. entomon*, on the other hand, the position of the germ cells is different in each testicular tubule; for instance, the peripheral part of the lumen of one tubule is mainly occupied by secondary spermatocytes, while in its center, young spermatids are abundant. The lumen of the second tubule contains no sign of secondary spermatocytes, but spermatids undergoing advanced stages of spermiogenesis are abundant. The third tubule only contains immature spermatozoa (Hryniewiecka-Szyfter and Tyczewska 1991; Hryniewiecka-Szyfter et al. 1999).

In *Ranina ranina*, primary spermatogonia are often seen interspersed with secondary spermatogonia and primary spermatocytes (Minagawa et al. 1994). In mysids, primary spermatogonia are found in the testicular cord, whereas secondary spermatogonia are in the center (Kasaoka 1974). In *S. entomon*, spermatogonia occupy only a narrow portion along the

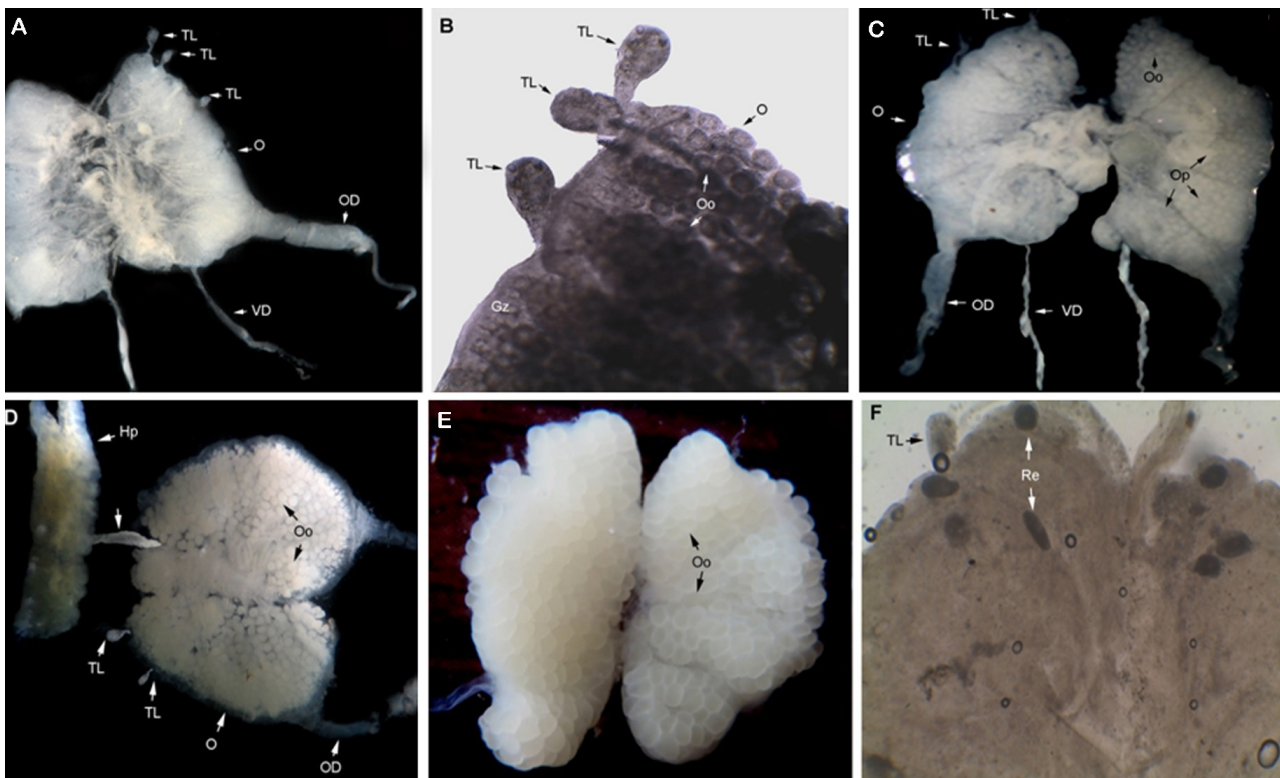


Fig. 8. *Mothocya renardi* (Bleeker, 1857): Reproductive system during the female phase. A, Ovary during the previtellogenic stage (4X); B, ovary during the previtellogenic stage showing oocytes (10X); C, ovary at Vg1 (4X); D, ovary at Vg2 connected with hepatopancreas (4X); E, ovary at Vg4 (4X); F, ovary during the spent stage (4X). O: ovary, TL: testis lobe, OD: oviduct, VD: vas deferens, Oo: oocyte, Gz: germinal zone, Op: ovarian pouch, Hp: hepatopancreas, Re: residual oocytes.

bottom of the testicular tubule, forming a compact cell pattern characterized by a large nucleus and nucleolus (Hryniewiecka-Szyfter and Tyczewska 1991). In *M. renardi* the secondary spermatogonia are smaller than the primary ones, with an oval nucleus in which chromatin granules display a homogenous distribution unlike that of primary spermatogonia, the nucleus of which contains peripheral chromatin. In *M. renardi* both spermatocytes and early-stage spermatids are

characterized by the presence of a large round nucleus with condensed chromatin. The spermatids with various, more advanced stages of spermiogenesis are also common in the testis lumen of *M. renardi*.

The morphology and ultrastructure of the spermatozoa and spermatophores in the testes and vas deferens of *M. renardi* appear to be similar to those described in *N. indica* (Kottarathil and Kappalli 2019a) and species of free-living isopods (Hryniewiecka-

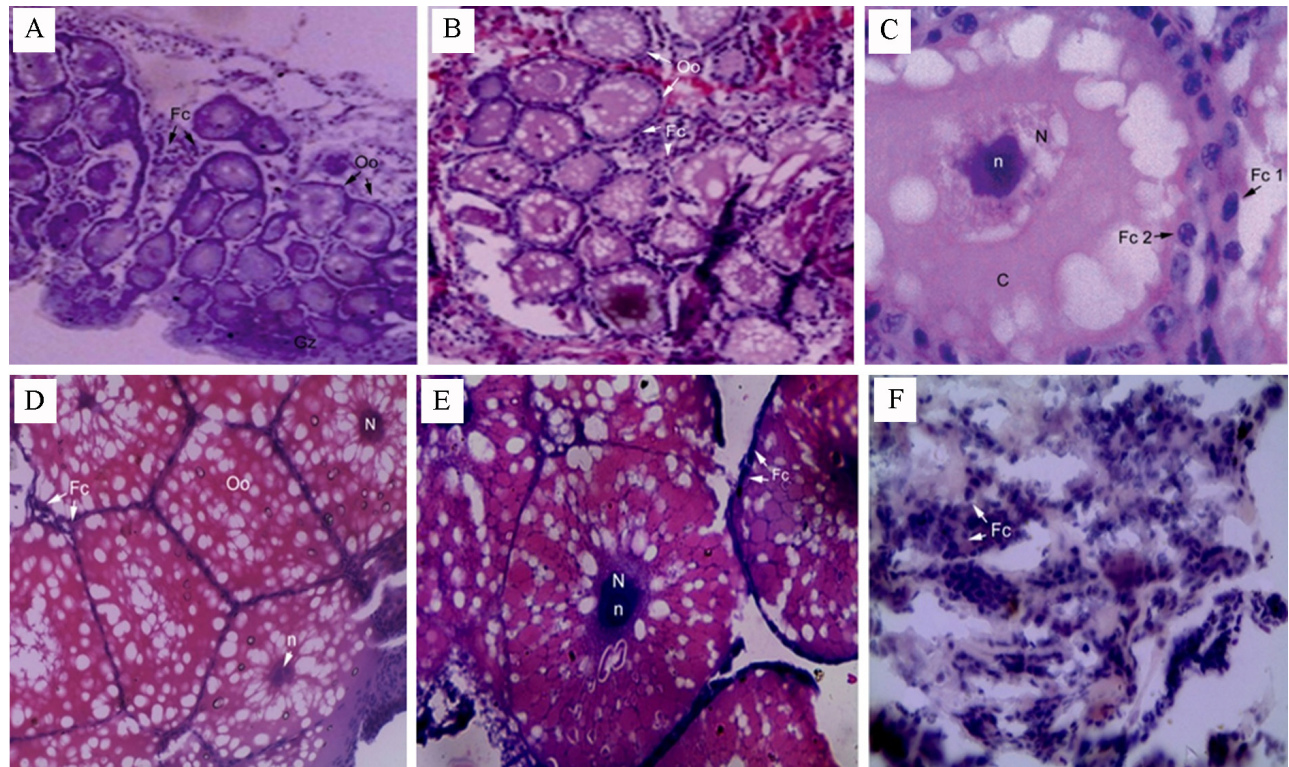


Fig. 9. *Mothocya renardi* (Bleeker, 1857): Histological section of the ovary during the female stage. A, previtellogenic stage showing germinal zone and previtellogenic oocytes (20X); B, Vg1 stage (10X); C, Vg1 oocytes showing nucleus and follicle cells (100X); D, Vg3 oocytes (10X); E, Vg5 (4X); F, spent stage (40X). Oo: oocyte, Gz: germinal zone, N: nucleus, n: nucleolus, Fc: follicle cells, Fc1: follicle cell - 1, Fc2: follicle cell - 2, C: cytoplasm.

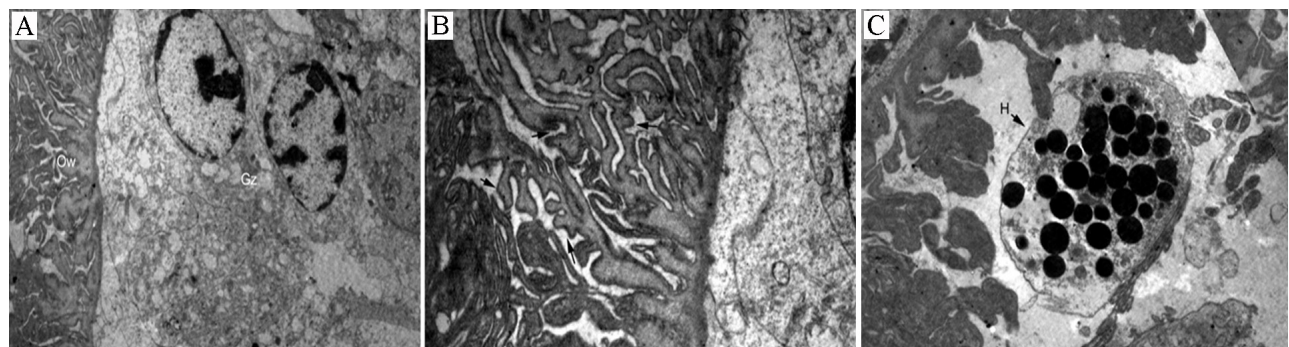


Fig. 10. *Mothocya renardi* (Bleeker, 1857): Electron micrograph of the ovary during the previtellogenic stage. A, germinal zone (2900X); B, highly convoluted (arrows) ovarian wall (6800X); C, haemocytes in the ovary (4800X). Ow: ovarian wall, Gz: germinal zone, H: haemocytes.

Szyfter and Tyczewska 1991). Each spermatophore is formed by a bundle of spermatozoa whose number varies from species to species. In *M. renardi* the number of spermatozoa in each bundle ranges from 66 to 106. In *S. entomon*, a spermatophore contains an average of 30 spermatozoa. In the oniscid isopods *Armadillidium vulgare* (Latreille, 1804) and *A. peraccae*, the average is 22 and 35, respectively. In *M. renardi* the sperm bundle formation seems to be completed within the testis lobes before being ejected out into the ovarian lobe and finally accumulating in the vas deferens, and their transport seems to be facilitated by the contraction of the muscular walls of the testis and ovary. In this cymothoid, the lumen contains spermatophores throughout the vas deferens, irrespective of regional morphological differences. In the spermatophore, spermatozoa lie parallel to one another, akin to the spermatozoa of *S. entomon* and *N. indica* (Hryniewiecka-Szyfter and Tyczewska 1991; Kottathil and Kappalli 2019a). In *M. renardi*, each spermatozoan bundle in both testes and vas deferens is enclosed by a fine granular matrix and assembly of longitudinally aligned extra tubular structures resembling the pattern described in *A. peraccae* and *N. indica* (Trovato et al. 2011; Kottathil and Kappalli 2019a). Longitudinally-aligned extra tubular structures are also visible, enclosing the individual spermatozoon in the spermatozoan bundles throughout its entire length, signifying the importance of the tubular system in spermatophore formation in cymothoids.

In *M. renardi*, though previtellogenic oocytes have been shown to possess a large nucleus with one or two nucleoli, they did not change in size, shape, appearance, or number until transforming into the transitional

stage, agreeing the report on *N. indica* (Kottathil and Kappalli 2019a). According to Charniaux-Cotton and Payen (1985), oocytes stay in the male stage under the androgenic hormones on the secondary vitellogenesis. Khalaila and Sagi (1997) demonstrated that ablation of the androgenic gland in the intersexed males of the parastacid crayfish *Cherax quadricarinatus* von Martens, 1868 resulted in an increase in the gonadosomatic index of the ovarian component. Rudolph (1997) commented that the coexistence of oviducts and vas deferens in males of *Parastacus pugnax* Poepfig, 1835 challenges the control that the androgenic gland exerts over sex determination in Malacostraca. Implants of the androgenic gland after the fourth post embryonic molt in females of *Armadillidium vulgare* Latreille, 1804 do not inhibit oviduct development (Hasegawa et al. 1993). To explain the development of the ovary and oviduct in males of *M. renardi*, further studies are needed on the development of the androgenic gland and its role in sex reversal.

As reported in *N. indica* (Kottathil and Kappalli 2019a), by the onset of the transitional phase in *M. renardi*, all the previtellogenic oocytes have begun to grow synchronously and in parallel with active yolk deposition. During this phase, late-stage ovaries (oocyte size approximately 1100 μm) are very common. The extremity of the oviduct, however, remains closed until it transforms into functional females through the parturial molt.

In the functional ovigerous females of *M. renardi*, the kidney-shaped and paired ovaries appear to be the same size. Contrary to this, in non-hermaphroditic oniscid isopods, the paired ovaries are rarely the same

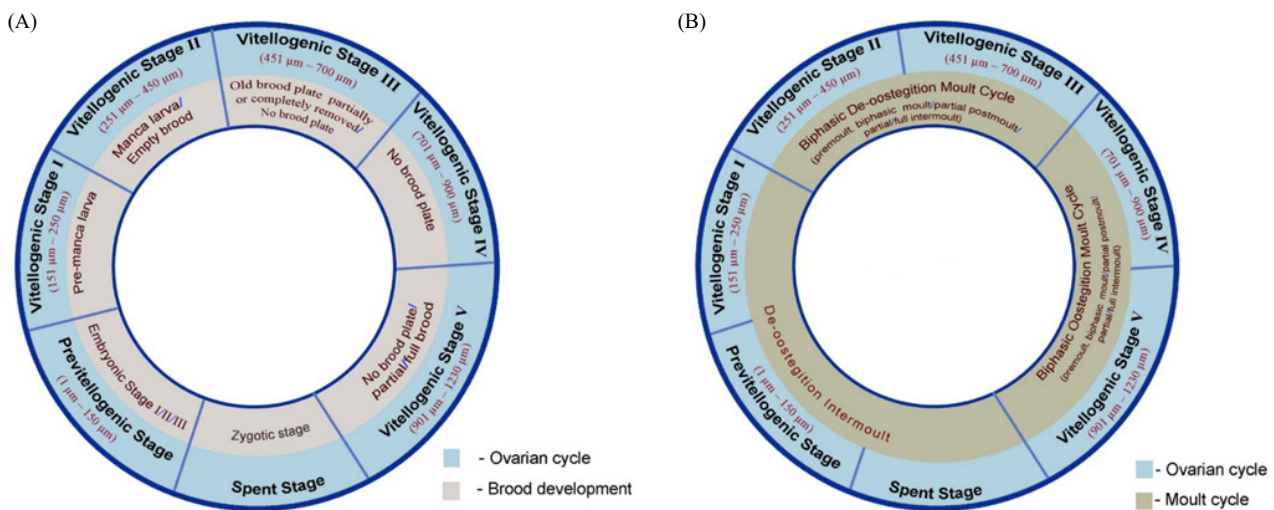


Fig. 11. *Mothocya renardi* (Bleeker, 1857): Female stage. Correlation between (A) ovarian cycle and brood development; (B) ovarian cycle and molt cycle.

size (Warburg 2013). Apart from the paired ovary and oviducts, the gonad of the isopod *S. entomon* is characterized by the presence of a fertilization chamber and paired spermatheca (Hryniewiecka-Szyfter and Tyczewska 1992). Furthermore, in this species, the wall of the proximal part, close to the germinative zone, is composed of an epithelium and follicle cells, while that of the distal part is built of an epithelium surrounded by a muscular layer (Hryniewiecka-Szyfter and Babula 1995). Such a regional difference in the wall of the ovary was not prominent in *M. renardi*. Ultrastructurally, the previtellogenic ovary wall of *M. renardi* contains copious festoon-shaped convolutions towards the lumen of the ovary. Furthermore, the ovarian lobe during the subsequent stage contained 10–12 cone-shaped ovarian pouches, each containing the oocytes more or less at the same stage of yolk deposition. A similar pattern of ovarian structure has been reported in shrimps, crayfishes, and brachyuran crabs (Krol et al. 1992; Ando and Makioka 1999; Holdich 2002; Meeratana and Sobhon 2007), but not in the ovary of *N. indica* (Kottarathil and Kappalli 2019b).

The ovary of *M. renardi* during its female stage undergoes sequential morphological and cytological changes during the ovarian cycle. Seven ovary stages were identified based on the gross morphology, oocyte size, and coloration. Oocytes in Pvs usually appear with a large nucleus and one or two visible nucleoli, akin to those described in *S. entomon* and *P. scaber* (Bilinski 1979; Hryniewiecka-Szyfter and Babula 1995). The yolky oocytes of *M. renardi* contain a large nucleus, nucleoli, and encircled follicles during stages Vg1–5.

The population of *M. renardi* in the present study did not exhibit any degree of synchrony in its breeding pattern, presumably due to its hermaphroditic and obligatory parasitic traits akin to the reports in *N. indica* (Kottarathil and Kappalli 2019b). Nevertheless, our close observations revealed the existence of a perfect and remarkable synchrony between the ovarian stages and developmental stages of the egg incubated in the marsupium among individuals. This characteristic feature enables us to evaluate and predict the ovarian stages of live parasites without sacrificing them.

The interrelationship between molting and female reproduction has been demonstrated in several other crustacean species. Like the observation made in *M. renardi*, the synergistic programming of growth and reproduction has also been well demonstrated in isopods like *A. vulgare*, *Idotea balthica*, and *N. indica*, and shrimps and fiddler crabs (Souty 1980; Souty and Picaud 1981; Suzuki et al. 1990; Okumura 2004; Sudha et al. 2012; Kottarathil and Kappalli 2019b). Interestingly, in *M. renardi*, each ovarian cycle is accompanied by two molting cycles, signifying a

remarkable degree of synergism between molting and reproduction, supporting the pattern reported in *N. indica* (Kottarathil and Kappalli 2019b).

CONCLUSIONS

The present study gives morphological, histological, and ultrastructural evidence of sequential protandrous hermaphroditic changes in the reproductive system of the cymothoid *Mothocya renardi* while it passes through male, transitional, and female phases. During the male phase, the inner cores of testes lobes were occupied by germ cells undergoing spermatogenesis and spermeogenesis and the outer cores were filled with primary and secondary spermatogonial cells. Similarly, the ovary was centered with a large number of yolky oocytes encircled by follicle cells. Oviduct opens from the mid-lateral ovary, but its distal end was closed. The exceptionally elongated spermatozoa organized into a bundle called spermatophores were found packed in the ovary as well as in the vas deferens. Conversely, during the transitional phase, testes appeared withered, but the vas deferens and ovary accommodated spermatophores and yolky oocytes, respectively. During the female phase, the testis lobes appear as thin, empty and sac like and the vas deferens aperture is closed. Ovaries contain yolky oocytes and oviducts more prominent. It is also understood that, in *M. renardi*, each ovarian cycle is accompanied by two molting cycles. All of this basic information will pave the way for in-depth studies on the physiological and molecular mechanisms of protandrous hermaphroditism in cymothoids.

Acknowledgments: SK gratefully acknowledges the University Grants Commission, New Delhi [F.No:38-218/2009(SR) dated 24/12/2009], Kerala State Council for Science, Technology and Environment, Government of Kerala [(No. (T) 093/SRS/2011/CSTE dated 25/06/2011 & KSCSTE/5224/2017-SRSLs dated 28.8.2018], and the Department of Science and Technology, Govt. of India (DST-SERB: EMR/2016/001163 dated 28.8.2017) for their financial support. We thank the two reviewers for their rigorous reviewing and for making the manuscript presentable. Noah Last of Third Draft Editing edited the manuscript's English.

Authors' contributions: APT worked on the topic of the study as the project fellow under a research project funded by the University Grants Commission, New Delhi [F.No:38-218/2009(SR) dated 24/12/2009]. SK, the Principal Investigator of the project and PhD mentor

of APT, drew out the concept, supervised the work, interpreted the results, and prepared the manuscript.

Competing interests: AP and SK declare that they have no conflict of interest.

Availability of data and materials: Voucher specimens are deposited in the collections of the Parasitic Crustacean Museum (PCM), Crustacean Biology Research Laboratory, Sree Narayana College, Kannur, Kerala, India.

Consent for publication: Not applicable.

Ethics approval consent to participate: The animals used in this study did not require ethical approval to experiment on.

REFERENCE

- Almeida AO, Buckup L. 1997. Aspectos anatômicos e funcionais do aparelho reprodutor de *Parastacus brasiliensis* (von Martens) (Crustacea, Decapoda, Parastacidae). *Rev Bras Zool* **14**:497–509. doi:10.1590/S0101-81751997000200017.
- Ando H, Makioka T. 1999. Structure of the ovary and mode of oogenesis in a freshwater crab *Potamon dehaani*. *J Morphol* **23**:107–114. doi:10.1002/(SICI)1097-4687(199901)239:1<107::AID-JMOR8>3.0.CO;2-j.
- Aneesh PT, Kappalli S. 2020. Occurrence of life cycle dependent monophasic and biphasic molting in a parasitic isopod *Mothocya renardi*. *Thalassas* **36**:115–124. doi:10.1007/s41208-019-00188-6.
- Aneesh PT, Kottarathil HA, Kappalli S. 2016. Branchial cymothoids infesting the marine food fishes of Malabar coast. *J Parasitic Dis* **40**:1270–1277. doi:10.1007/s12639-015-0666-0.
- Aneesh PT, Sudha K, Helna AK, Anilkumar G. 2018. *Agarna malayi* Tiwari 1952 (Crustacea: Isopoda: Cymothoidae) parasitizing the marine fish, *Tenualosa toli* (Clupeidae) from India: re-description/description of parasite life cycle and patterns of occurrence. *Zool Stud* **57**:25. doi:10.6620/ZS.2018.57-25.
- Bilinski S. 1979. Ultrastructural study of yolk formation in *Porcellio scaber* Latr Isopoda. *Cytobios* **26**:123–130.
- Brook HJ, Rawlings TA, Davies RW. 1994. Protogynous sex change in the intertidal isopod *Gnorimosphaeroma oregonense* Crustacea: Isopoda. *Biol Bull* **187**:99–111.
- Brusca RC. 1981. A monograph on the Isopoda Cymothoidae Crustacea of the eastern Pacific. *Zool J of Linnean Soc* **73**:117–199. doi:10.1111/j.1096-3642.1981.tb01592.x.
- Charniaux-Cotton H, Payen G. 1985. Sexual Differentiation. In: Bliss DE and L H Mantel eds *The Biology of Crustacea 9 Integument Pigments and Hormonal Processes*, Academic Press New York, pp. 217–299.
- Cook C, Munguia P. 2015. Sex change and morphological transitions in a marine ectoparasite. *Mar Ecol* **36**(3):337–346. doi:10.1111/maec.12144.
- Cotelli F, Ferraguti M, Lanzavecchia G, Donin CL. 1976. The spermatozoon of peracarida. I. The spermatozoon of terrestrial isopods. *J Ultrastruct Res* **55**:378–390. doi:10.1016/S0022-5320(76)80094-9.
- Cressey RF. 1983. Crustaceans as parasites of other organisms. In: *The biology of Crustacea* (pp. 251–273). Academic Press.
- Erkan BM. 1998. Ultrastructural Study on the Ovarian Wall and the Oviduct of the *Asellus aquaticus* Crustacea: Isopoda. *Turk J Zool* **22**:351–362.
- Hasegawa Y, Hirose E, Katakura Y. 1993. Hormonal control of sexual differentiation and reproduction in Crustacea. *Am Zool* **33**:403–411. doi:10.1093/icb/33.3.403.
- Holdich DM. 2002. *Biology of Freshwater Crayfish*. Blackwell Science Ltd, Osney Mead, Oxford, 702 pp.
- Hryniewiecka-Szyfter Z, Babula A. 1995. Ultrastructural study of the female reproductive system of *Saduria entomon* (Linnaeus, 1758) (Isopoda, Valvifera). *Crustaceana* **6**(86):720–733. doi:10.1163/156854095X00232.
- Hryniewiecka-Szyfter Z, Gabala E, Babula A. 1999. The role of Sertoli cells in the organization of sperm bundles in the testis of *Saduria entomon* (Linnaeus, 1758) (Isopoda, Valvifera). *Crustaceana* **72**:1067–1078. doi:10.1163/156854099504022.
- Hryniewiecka-Szyfter Z, Tyczewska J. 1991. The Histology of the Male Reproductive System of *Saduria entomon* (Linnaeus, 1758) (Isopoda, Valvifera). *Crustaceana* **60**(3):246–257. doi:10.1163/156854091X00038.
- Hryniewiecka-Szyfter Z, Tyczewska J. 1992. Morphological organization of the female reproductive system of *Saduria entomon* (Linnaeus, 1758) (Isopoda, Valvifera). *Crustaceana* **63**:1–10. doi:10.1163/156854092X00226.
- Itaya PW. 1979. Microscopic investigation of the formation of spermatophores of *Armadillidium vulgare*. *Cell Tissue Res* **196**:95–102.
- Kasaoka LD. 1974. The male genital system in two species of mysid Crustacea. *J Morphol* **143**:259–284. doi:10.1002/jmor.1051430303.
- Khalaila I, Sagi A. 1997. Intersexuality and its control by the androgenic gland in the crayfish *Cherax quadricarinatus*. *J Reprod Develop* **43**:69–70.
- Kottarathil HA, Kappalli S. 2019a. Reproductive system in the male phase of a parasitic Isopod Crustacea-morphological histological and ultrastructural evidence for sequential protandrous hermaphroditic changes. *Zool Stud* **58**:4. doi:10.6620/ZS.2019.58-04.
- Kottarathil HA, Kappalli S. 2019b. Characterization of a protandrous hermaphroditic reproductive system in transitional and female phases of *Norileca indica* — morphological, histological and ultrastructural approach. *Crustaceana* **92**:641–664. doi:10.1163/15685403-00003896.
- Krol RM, Hawkins WE, Overstreey RM. 1992. Reproductive components. In: F. W. Harrison, and A. G. Humes (eds.), *Microscopic Anatomy of Invertebrates*. Vol. 10. Wiley-Liss Inc New York, pp. 295–343.
- Legrand JJ. 1952. Contribution à l'étude expérimentale et statistique de la biologie d'Anilocra physodes L. (Crustacé Isopode Cumothordé). *Arch Zool expér gén* **89**:1–55, Paris, France.
- Meeratana P, Sobhon P. 2007. Classification of differentiating oocytes during ovarian cycle in the giant freshwater prawn *Macrobrachium rosenbergii* de man. *Aquaculture* **270**:249–258. doi:10.1016/j.aquaculture.2007.03.009.
- Minagawa MJR, Chiu MC, Takashima F. 1994. Male reproductive biology of the red frog crab *Ranina ranina* off Hachijojima Izu Inlands Japan. *Mar Biol (Berlin)* **118**:393–401.
- Okumura T. 2004. Perspectives on hormonal manipulation of shrimp reproduction. *JPN AGR Res* **38**:49–54. doi:10.6090/jarq.38.49.
- Pearse AGE. 1968. *Histochemistry: theoretical and applied 3rd ed* Vol I. Little Brown and Co Boston 759 pp.
- Poulin R. 1995. Evolutionary influences on body size in free-

- living and parasitic isopods. Biol J of Linn Soc **54**:231–244. doi:10.1111/j.1095-8312.1995.tb01035.x.
- Reger JF, Fain-Maurel M. 1973. A comparative study on the origin, distribution, and fine structure of extracellular tubules in the male reproductive system of species of isopods, amphipods, schizopods, copepods, and cumacea. J Ultrastruct Res **44**:235–252. doi:10.1016/S0022-5320(73)80058-9.
- Reger JF, Itaya PW, Fitzgerald ME. 1979. A thin section and freeze-fracture study of membrane specializations in spermatozoa of the isopod. *Armadillidium vulgare*. J Ultrastruct Res **67**:180–193. doi:10.1016/S0022-5320(79)80006-4.
- Rudolph EH. 1997. Intersexualidad en el camarón excavador *Parastacus pugnax* (Poeppig, 1835) (Decapoda, Parastacidae). Investig Mar **25**:7–18. doi:10.4067/S0717-71781997002500002.
- Rudolph EH. 1999. Intersexuality in the freshwater crayfish *Samastacus spinifrons* (Philippi, 1882) (Decapoda, Parastacidae). Crustaceana **72**:325–337. doi:10.1163/156854099503401.
- Shuster SM, Wade MJ. 1991. Equal mating success among male reproductive strategies in a marine isopod. Nature **350**:608–610. doi:10.1038/350608a0.
- Shuster SM, Wade MJ. 2003. Mating system and strategies. Princeton University Press, UK.
- Smit N, Bruce N, Hadfield K. 2019. Introduction to Parasitic Crustacea: State of Knowledge and Future Trends. In: Smit N., Bruce N., Hadfield K. (eds) Parasitic Crustacea, pp. 1–6. Zoological Monographs, vol. 3. Springer, Cham. doi:10.1007/978-3-030-17385-2_1.
- Souty C. 1980. Electron microscopic study of follicle cell development during vitellogenesis in the marine crustacean Isopoda, *Idotea balthica basteri*. Reprod Nutr Dev **20**:653–663. doi:10.1051/rnd:19800407.
- Souty C, Picaud JL. 1981. Vitellogenin synthesis in the fat body of the marine crustacean Isopoda, *Idotea balthica basteri*, during vitellogenesis. Reprod Nutr Dev **21**:95–101. doi:10.1051/rnd:19810108.
- Sudha K, Supriya NT, Anilkumar G, Chang ES. 2012. Hemolymph ecdysteroid titres in a brachyuran crab *Uca triangularis* that concomitantly undergoes molting and reproduction. Zool Stud **51**:966–976.
- Suzuki S, Yamasaki K, Katakura Y. 1990. Vitellogenin synthesis in andrectomized males of the terrestrial isopod, *Armadillidium vulgare* (Malacostracan Crustacea). Gen Comp Endocrinol **772**:283–291. doi:10.1016/0016-6480(90)90312-A.
- Trovato M, Mazzeia V, Sinatrab F, Longo G. 2011. Presence of F-actin in sperm head of *Armadillidium peraccae* (Isopoda, Oniscidea). Tissue Cell **43**:304–310. doi:10.1016/j.tice.2011.06.002.
- Tsai ML, Dai CF. 1999. *Ichthyoxenus fushanensis*. new species (Isopoda: Cymothoidae), parasite of the fresh-water fish *Varicorhinus bacbatulus* from northern Taiwan. J Crustacean Biol **19**:917–923. doi:10.1163/193724099X00600.
- Tsai ML, Li JJ, Dai CF. 1999. Why selection favors protandrous sex change for the parasitic isopod *Ichthyoxenus fushanensis* Isopoda: Cymothoidae. Evol Ecol **13**:327–338.
- Warburg MR. 2013. Post-parturial reproduction in terrestrial isopods: a partial review. Invertebr Reprod Dev **571**:10–26. doi:10.1080/07924259.2011.633620.
- Williams DB, Carter CB. 1997. Transmission Electron Microscopy—a text book for material science. Micron **281**:75–75.